

## Thermal diffusivity of nonflat plates using the flash method

Agustín Salazar,<sup>a)</sup> Raquel Fuente, Estibaliz Apiñaniz, and Arantza Mendioroz  
*Departamento de Física Aplicada I, Escuela Técnica Superior de Ingeniería, Universidad del País Vasco,  
 Alameda Urquijo s/n, 48013 Bilbao, Spain*

(Received 25 September 2010; accepted 21 November 2010; published online 25 January 2011)

The flash method is the standard technique to measure the thermal diffusivity of solid samples. It consists of heating the front surface of an opaque sample by a brief light pulse and detecting the temperature evolution at its rear surface. The thermal diffusivity is obtained by measuring the time corresponding to the half maximum of the temperature rise, which only depends on the sample thickness and thermal diffusivity through a simple formula. Up to now, the flash method has been restricted to flat samples. In this work, we extend the flash method to measure the thermal diffusivity of nonflat samples. In particular, we focus on plates with cylindrical and spherical shapes. The theoretical model indicates that the same expression for flat samples can also be applied to cylindrical and spherical plates, except for extremely curved samples. Accordingly, a curvature limit for the application of the expression for flat samples is established. Flash measurements on lead foils of cylindrical shape confirm the validity of the model. © 2011 American Institute of Physics. [doi:10.1063/1.3529431]

### I. INTRODUCTION

The flash method is the most acknowledged technique to measure the thermal diffusivity. In many countries, it is currently considered as a standard for thermal diffusivity measurements of solid materials. It was introduced by Parker and coworkers and consists of heating the front face of an opaque plate by a brief light pulse and detecting the temperature evolution at its rear face.<sup>1</sup> The thermal diffusivity is obtained by measuring the time corresponding to the half maximum of the temperature rise ( $t_{1/2}$ ), which is related to the thermal diffusivity through the expression,

$$t_{1/2} = 0.1388 \frac{L^2}{D}, \quad (1)$$

where  $L$  is the sample thickness and  $D$  is the thermal diffusivity. This procedure works under ideal conditions: uniform illumination, negligible pulse duration, and negligible heat losses. When these requirements are not fulfilled, a fit to the complete temperature history of the rear surface must be performed.

Up to now, the flash method has been mainly restricted to flat samples. In the last years, the flash method has been used to measure the radial thermal diffusivity of rods, tubes, and spheres.<sup>2,3</sup> In this work, we extend the classical flash method to measure the thermal diffusivity of nonflat plates. In particular, we focus on plates with cylindrical and spherical shapes. First, we develop a theoretical model to calculate the temperature rise above the ambient at the rear surface of cylindrical and spherical plates illuminated by a uniform and brief light pulse. Numerical simulations indicate that the effect of the curvature is almost negligible, in such a way that Eq. (1) can be directly used except for extremely curved samples. A curvature limit to apply Eq. (1) is established. Flash measurements of the back surface temperature of cylindrical lead foils confirm the validity of the model.

<sup>a)</sup>Electronic mail: agustin.salazar@ehu.es.

### II. THEORETICAL MODEL

The theoretical model is developed in two steps. First, we recall the calculation of the temperature rise above the ambient of a flat plate illuminated by a brief light pulse. Then, we extend this calculation to the case of cylindrical and spherical plates.

#### A. Background: A flat plate

Let us consider an opaque flat plate of thickness  $L$  uniformly illuminated by an ideal Dirac pulse whose energy density is  $Q_o$  ( $J/m^2$ ). Its cross-section is shown in Fig. 1(a). To obtain the time evolution of this sample, we need to solve the one-dimensional heat diffusion equation, which in the absence of heat sources writes

$$\frac{\partial^2 T}{\partial x^2} - \frac{1}{D} \frac{\partial T}{\partial t} = 0. \quad (2)$$

Along this work  $T$  represents the temperature rise above the ambient. Its Laplace transform is

$$\frac{d^2 \bar{T}}{dx^2} - q^2 \bar{T} = 0, \quad (3)$$

where  $q^2 = s/D$ , being  $s$  the Laplace variable and  $\bar{T}$  the Laplace transform of the temperature rise. The general solution of Eq. (3) writes

$$\bar{T}(x, s) = A \sinh(qx) + B \cosh(qx), \quad (4)$$

where  $A$  and  $B$  are constants to be obtained from the boundary conditions, which in the absence of heat losses are

$$\Phi(x=0) = -K \left. \frac{dT}{dx} \right|_{x=0} = Q_o \delta(t), \quad (5a)$$

$$\Phi(x=L) = -K \left. \frac{dT}{dx} \right|_{x=L} = 0, \quad (5b)$$

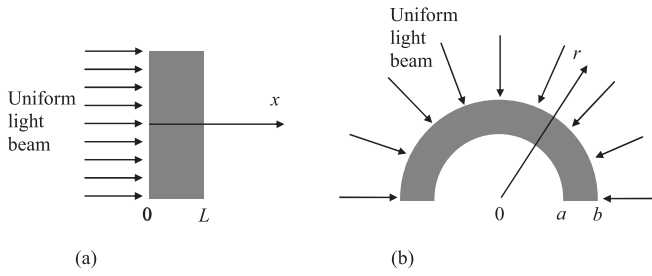


FIG. 1. Cross-section of: (a) a flat plate and (b) a cylindrical or spherical plate.

where  $K$  is the thermal conductivity of the plate and  $\delta(t)$  is the Dirac Delta function. The Laplace transforms of Eqs. (5) are

$$\bar{\Phi}(x=0) = -K \left. \frac{d\bar{T}}{dx} \right|_{x=0} = Q_o, \quad (6a)$$

$$\bar{\Phi}(x=L) = -K \left. \frac{d\bar{T}}{dx} \right|_{x=L} = 0. \quad (6b)$$

By substituting Eq. (4) into Eqs. (6), the Laplace transform of the temperature at any point of the plate is obtained

$$\bar{T}(x, s) = \frac{Q_o}{Kq} \frac{\cosh(qL)\cosh(qx) - \sinh(qL)\sinh(qx)}{\sinh(qL)}. \quad (7)$$

In particular, the value at the rear surface writes

$$\bar{T}(L, s) = \frac{Q_o}{Kq} \frac{1}{\sinh(qL)}. \quad (8)$$

By applying the inverse Laplace transform to these last equations, the time evolution of the plate temperature can be obtained. As there is not analytical solution for it, a numerical inversion must be performed, using, for instance, the Stehfest algorithm.<sup>4,5</sup>

It is worth mentioning that an analytical solution of the temperature of a flat and opaque plate after being heated by a Dirac pulse can be obtained [see, for instance, Eq. (2) in Ref. 1]. We have worked in Laplace space in order to introduce the method that will be used for cylindrical and spherical plates, for which no analytical solutions have been found.

## B. A cylindrical plate

Now we consider an opaque cylindrical plate of inner radius  $a$  and outer radius  $b$  uniformly illuminated by an ideal Dirac pulse with energy density  $Q_o$ . Its cross-section is shown in Fig. 1(b). The time evolution of the temperature of this sample is obtained by solving the heat diffusion equation in cylindrical coordinates, which due to the cylindrical symmetry writes

$$\frac{\partial^2 T}{\partial r^2} + \frac{1}{r} \frac{\partial T}{\partial r} - \frac{1}{D} \frac{\partial T}{\partial t} = 0, \quad (9)$$

whose Laplace transform is

$$\frac{d^2 \bar{T}}{dr^2} + \frac{1}{r} \frac{d\bar{T}}{dr} + q^2 \bar{T} = 0, \quad (10)$$

where  $q^2 = -s/D$ . The general solution of Eq. (10) writes<sup>6</sup>

$$\bar{T}(r, s) = A J_0(qr) + B H_0(qr), \quad (11)$$

where  $J_0$  and  $H_0$  are the Bessel and Hankel functions of zeroth order. As before,  $A$  and  $B$  are constants to be determined from the boundary conditions, which in the absence of heat losses are

$$\Phi(r=a) = -K \left. \frac{dT}{dr} \right|_{r=a} = 0, \quad (12a)$$

$$\Phi(r=b) = K \left. \frac{dT}{dr} \right|_{r=b} = Q_o \delta(t). \quad (12b)$$

Their Laplace transforms are

$$\bar{\Phi}(r=a) = -K \left. \frac{d\bar{T}}{dr} \right|_{r=a} = 0, \quad (13a)$$

$$\bar{\Phi}(r=b) = K \left. \frac{d\bar{T}}{dr} \right|_{r=b} = Q_o. \quad (13b)$$

By substituting Eq. (11) into Eqs. (13), the Laplace transform of the temperature at any point of the cylindrical plate is obtained,

$$\bar{T}(r, s) = \frac{Q_o}{Kq} \frac{J_1(qa)H_0(qr) - H_1(qa)J_0(qr)}{J_1(qb)H_1(qa) - H_1(qb)J_1(qa)}. \quad (14)$$

As before, the Stehfest algorithm can be used to invert Eq. (14) numerically in order to obtain the temperature history of the cylindrical plate after the flash pulse.

## C. A spherical plate

In a similar way, we study an opaque spherical plate of inner radius  $a$  and outer radius  $b$  uniformly illuminated by an ideal Dirac pulse whose energy density is  $Q_o$ . Its cross-section is shown in Fig. 1(b). The heat diffusion in spherical coordinates with spherical symmetry writes

$$\frac{\partial^2 T}{\partial r^2} + \frac{2}{r} \frac{\partial T}{\partial r} - \frac{1}{D} \frac{\partial T}{\partial t} = 0, \quad (15)$$

whose Laplace transform is

$$\frac{d^2 \bar{T}}{dr^2} + \frac{2}{r} \frac{d\bar{T}}{dr} + q^2 \bar{T} = 0, \quad (16)$$

where  $q^2 = -s/D$ . The general solution of Eq. (16) is<sup>7</sup>

$$\bar{T}(r, s) = A j_0(qr) + B h_0(qr), \quad (17)$$

where  $j_0$  and  $h_0$  are the spherical Bessel and Hankel functions of zeroth order. Following the same procedure as in the previous subsection, constants  $A$  and  $B$  are obtained from the boundary conditions. In this way, the Laplace transform of the temperature at any point of the spherical plate is obtained

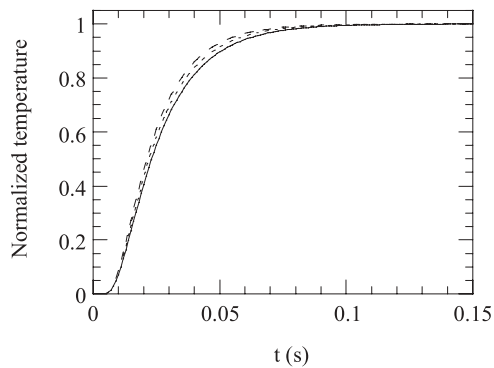


FIG. 2. Temperature history of the rear surface of a lead foil 2 mm thick after the absorption of an instantaneous flash pulse: A flat foil (continuous line), a cylindrical foil with an inner radius of 1 mm and an outer radius of 3 mm (dotted line), and a spherical foil with the same radii (dashed line). The inset shows the shape of the curvature.

$$\bar{T}(r, s) = \frac{Q_o j_1(qa)h_0(qr) - h_1(qa)j_0(qr)}{Kq j_1(qb)h_1(qa) - h_1(qb)j_1(qa)}. \quad (18)$$

Note that Eq. (18) is the same as Eq. (14) but replacing the ordinary Bessel and Hankel functions (of integer order) by the spherical Bessel and Hankel functions (of fractional order).

### III. NUMERICAL SIMULATIONS

By applying the Stehfest algorithm to Eqs. (8), (14), and (18), we have calculated the rear surface temperature rise of flat, cylindrical, and spherical plates illuminated by an instantaneous flash pulse. We have studied plates with the same thickness but varying curvature. The curvature can be quantified by the ratio  $L/a$ , where  $L = b - a$ . Accordingly, the smaller (larger) the  $L/a$  value the smaller (larger) the curvature is. Surprisingly, the  $t_{1/2}$  value hardly varies with the curvature. Only for  $L/a > 0.5$ , the difference in  $t_{1/2}$  with respect to a flat plate exceeds 1%. In Fig. 2, we show the normalized temperature evolution of the rear surface of a lead ( $D = 24 \text{ mm}^2 \text{ s}^{-1}$ ,  $K = 35 \text{ W m}^{-1} \text{ K}^{-1}$ ) foil 2 mm thick after the absorption of an instantaneous flash pulse. The continuous line corresponds to a flat foil, the dotted line to a cylindrical foil with an inner radius of 1 mm, and an outer radius of 3 mm (i.e.,  $L/a = 2$ ) and the dashed line to a spherical foil of the same radii. As can be seen, even for this extreme curvature, which is shown in the inset, the difference with respect to the flat plate is small. In Fig. 3, we show the overestimation of the thermal diffusivity of cylindrical and spherical plates when using Eq. (1) as a function of the curvature  $L/a$ . As can be seen, only for  $L/a > 1$  the effect of the curvature cannot be neglected. This result indicates that the flash method can be used directly for nonflat surfaces unless the curvature is very pronounced.

Note that the calculations have been performed for adiabatic slabs. When heat losses are considered (conduction and convection to the surrounding gas and radiation), Eq. (1) cannot be applied directly, but a fit of the whole temperature curve must be performed. Anyway, the conclusion on the small influence of the curvature stays.

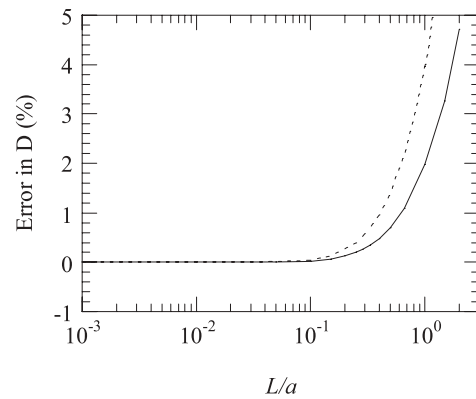


FIG. 3. Overestimation of the thermal diffusivity of a cylindrical plate (continuous line) and a spherical plate (dotted line) as a function of the curvature ( $L/a$ ).

### IV. EXPERIMENTAL RESULTS AND DISCUSSION

To validate the theoretical predictions, we have measured the rear surface temperature rise of several lead foils of the same thickness ( $L = 2.0 \text{ mm}$ ) but different curvatures. We have selected lead since due to its high ductility and malleability it can be easily shaped. Moreover, due to its high thermal conductivity the influence of heat losses can be neglected. The scheme of the experimental setup is shown in Fig. 4. The samples have been illuminated by two 3 kJ flash lamps and their rear surface temperature has been measured by an infrared video camera (JADE J550M from CEDIP) at a rate of 800 frames per second. A 50 mm lens has been used to collect the infrared emission from the sample surface. The lens is placed at its minimum working distance (23 cm) from the sample. In this way, each pixel measures the average temperature over a square of  $135 \mu\text{m}$  side on the back surface of the plate. Infrared filters in front of the flash lamps have been used to cut their infrared emission. A variable slit is placed around the sample in order to prevent direct light from reaching the detector.

Only the temperature at the center of the foil is recorded (see Fig. 4). There are two reasons for that: (a) due to the curvature of the sample only this point is focused on the detector array and (b) it is the region where the illumination is more homogeneous, as required by the theoretical model

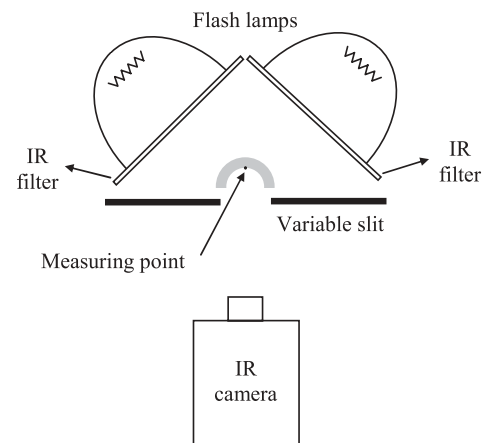


FIG. 4. Scheme of the experimental setup.

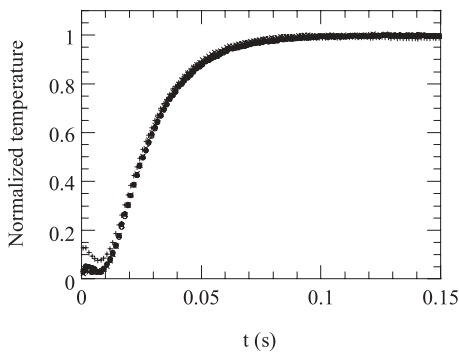


FIG. 5. Experimental evolution of the rear surface temperature of several lead foils 2.0 mm thick after being heated by two flash lamps. Foils of different curvatures have been measured:  $L/a = 0$  ( $\bullet$ ), 0.125 ( $\circ$ ), 0.20 ( $\times$ ), and 0.57 ( $+$ ).

[see Fig. 1(b)]. Both sides of the foils have been painted with a thin graphite layer (about  $10 \mu\text{m}$  thick) to increase both their absorption to the flash light and their infrared emission. Moreover, the black layer at the inner surface of the curved foil drastically reduces the multiple reflections of the emitted IR radiation, which could falsify the temperature field seen by the camera (especially for the sample with the largest curvature). The effect of this thin layer on the accuracy of the thermal diffusivity using the flash is less than 1% provided the sample is much thicker than the paint layer (in our case, 2 mm against  $20 \mu\text{m}$ ).<sup>8,9</sup>

We have measured the time evolution of the temperature at the center of the rear surface of lead foils with the following curvatures:  $L/a = 0$  (flat slab), 0.03, 0.125, 0.20, 0.33, and 0.57. The results are shown in Fig. 5. As they are almost coincident only the results for four of them are depicted. Each curve has been normalized to its maximum temperature rise in order to better compare the results. As can be seen, in all cases the asymptotic value is flat, indicating that heat losses are negligible. On the other hand, the shape of the curves is the same, within the experimental uncertainty, confirming the small effect of the curvature. Only for the largest curvature,  $L/a = 0.57$ , a small reduction of  $t_{1/2}$  takes place, as predicted by the theoretical model.

As we have used a quite thin slab for a so high thermal conducting material, the  $t_{1/2}$  values are quite short ( $t_{1/2}$

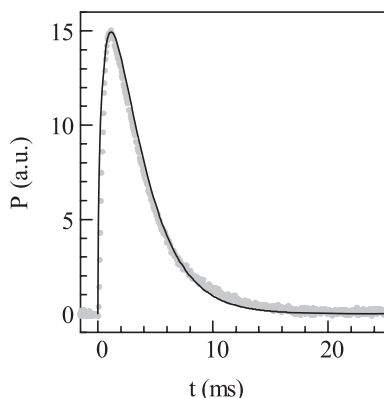


FIG. 6. Power distribution of the flash lamp. Dots are the experimental data, while the continuous line is the fit to an exponential law.

TABLE I. Thermal diffusivity values of lead slabs of different curvature. The experimental uncertainty is 3%.

$L/a$	$D$ ( $\text{mm}^2/\text{s}$ )
0	24.8
0.03	24.7
0.125	24.9
0.20	24.5
0.33	24.7
0.57	25.6

$\approx 0.026\text{s}$ ) and, therefore, the finite duration of the flash lamps cannot be neglected. Because of this finite duration of the flash pulse,  $t_{1/2}$  is longer than it would be for an instantaneous flash pulse. Accordingly, the thermal diffusivity of lead will be underestimated if Eq. (1) is used directly. This issue has been addressed by several authors.<sup>10–12</sup> We have measured the power distribution of our flash lamp for its six energy levels. It satisfies the following exponential law:  $P(t) = (Q_o/N)(t^\alpha/\tau^{1+\alpha}) \exp(-t/\tau)$ , where  $\alpha$  and  $\tau$  are parameters which depend on the energy of the flash lamp and  $N$  is a normalization constant in order to satisfy the condition  $\int_0^\infty P(t)dt = Q_o$ . The power distribution for the highest energy delivered by the flash lamp is shown in Fig. 6. Dots are the experimental data, while the continuous line is the fit to the exponential law with  $\alpha = 0.50$  and  $\tau = 0.0023$  s. The Laplace transform is  $\bar{P}(s) = Q_o/(1 + s\tau)^{1+\alpha}$ . Accordingly, the effect of the finite duration of the flash lamps is accounted for by substituting in Eqs. (7), (14), and (18)  $Q_o$  by  $Q_o/(1 + s\tau)^{1.5}$ . We have performed calculations for different values of  $\alpha$  and  $\tau$  for flat, cylindrical, and spherical plates and we can conclude that Eq. (1) can be used to retrieve the thermal diffusivity accurately provided  $t_{1/2} - \Delta t$  is used instead of  $t_{1/2}$ , where  $\Delta t = (1 + \alpha)\tau$ , in our case  $0.0034$  s.<sup>3</sup>

A final experimental remark deserves comment. For the sample with the largest curvature, we observed an increase of the roughness, together with the appearance of some small cracks, at the inner surface. This indicates that the lead reached the elasticity limit. That is the reason why we did not try measurements on foils with higher curvatures.

The thermal diffusivity values for the six Pb samples, we have measured are summarized in Table I. The uncertainty of the measurements is 3%. Only the value corresponding to the largest curvature slightly overestimates the lead diffusivity in excellent agreement with the prediction of the theoretical model. It is worth mentioning that although the model requires a uniform illumination of the curved samples the use of two flash lamps at right angle fulfils the uniformity condition.

In summary, in this paper we have demonstrated theoretically and experimentally that the flash method can be easily extended to nonflat plates provided their curvature, defined as the ratio between the thickness and the inner radius, is smaller than 0.5.

## ACKNOWLEDGMENTS

This work has been supported by the Ministerio de Educación y Ciencia (MAT2008-01454).

- <sup>1</sup>W. J. Parker, R. J. Jenkins, C. P. Buttler, and G. L. Abbott, *J. Appl. Phys.* **32**, 1679 (1961).
- <sup>2</sup>A. Salazar, F. Garrido, and R. Celorrio, *J. Appl. Phys.* **99**, 066116 (2006).
- <sup>3</sup>E. Apiñaniz, A. Mendioroz, N. Madariaga, A. Oleaga, R. Celorrio, and A. Salazar, *J. Phys. D: Appl. Phys.* **41**, 015403 (2008).
- <sup>4</sup>H. Stehfest, *Commun. ACM* **13**, 47 (1970).
- <sup>5</sup>D. Maillat, S. André, J. C. Batsale, A. Degiovanni, and C. Moyne, *Thermal Quadrupoles* (Wiley, New York, 2000).
- <sup>6</sup>A. Salazar and R. Celorrio, *J. Appl. Phys.* **100**, 113535 (2006).
- <sup>7</sup>N. Madariaga and A. Salazar, *J. Appl. Phys.* **101**, 103534 (2007).
- <sup>8</sup>D. Maillat, C. Moyne, and B. Rémy, *Int. J. Heat Mass Transfer* **43**, 4057 (2000).
- <sup>9</sup>F. Cernuschi, L. Lorenzoni, P. Bianchi, and A. Figari, *Infrared Phys. Technol.* **43**, 133 (2002).
- <sup>10</sup>J. A. Cape and G. W. Lehman, *J. Appl. Phys.* **34**, 1909 (1963).
- <sup>11</sup>R. E. Taylor and L. M. Clark III, *Appl. Phys. Lett.* **5**, 212 (1964).
- <sup>12</sup>T. Azumi and Y. Takahashi, *Rev. Sci. Instrum.* **52**, 1411 (1981).